Proceedings of the European Conference Physics of Magnetism, Poznań 2017

Magnetocaloric Effect in Antiferromagnetic Half-Heusler Alloy DyNiSb

K. Synoradzki*, K. Ciesielski and D. Kaczorowski

Institute of Low Temperature and Structure Research, Polish Academy of Sciences, Wrocław, Poland

The low-temperature magnetic, thermal and magnetocaloric properties of the half-Heusler compound DyNiSb were studied on polycrystalline samples. The temperature variations of the magnetization and the heat capacity revealed a phase transition from paramagnetic to antiferromagnetic state at the Néel temperature $T_{\rm N} = 3.1$ K. The compound exhibits normal and inverse magnetocaloric effect with the isothermal magnetic entropy change reaching 5.2 J/(kg K) at 4.8 K for a magnetic field change of 3 T. The estimated refrigerant capacity is about 58 J/kg.

DOI: 10.12693/APhysPolA.133.691

PACS/topics: 75.50.Ee, 75.30.Sg

1. Introduction

Magnetocaloric effect (MCE) in low-temperature regime is considered as a new refrigeration mechanism for liquefaction of gases like hydrogen and helium. Many Dy-based alloys and compounds show suitable magnetocaloric properties at temperatures $T < 20$ K [1–5].

DyNiSb is a member of the half-Heusler alloys family. It crystallizes with a cubic MgAgAs-type structure (space group $F\bar{4}3m$) and orders antiferromagnetically (AFM) below $T_{\rm N} = 3.5$ K with a propagation vector $\boldsymbol{q} = (0.5, 0.5, 0.5)$ [6]. The compound is a semiconductor and exhibits high magnetoresistance (MR) at low temperatures [7, 8], which may imply sizable MCE [9]. Above room temperature, the material shows large Seebeck coefficient [10]. In this paper we report on the magnetocaloric behaviour in DyNiSb assessed by means of magnetic measurements.

2. Experiment details

Ingot of DyNiSb was prepared by arc-melting stoichiometric amounts of the constituent elements (Dy 99.9 wt.%, Ni 99.999 wt.%, Sb 99.99 wt.%) on a water-cooled copper hearth under protective Ti-gettered argon atmosphere. To ensure homogeneity, the sample was turned over and re-melted three times. Subsequently, the button was sealed in an evacuated silica tube and annealed at 1000 K for 4 days.

Quality of the synthesized material was examined at room temperature by X-ray powder diffraction using an Xpert Pro PANalytical X-ray diffractometer with Cu K_α radiation. The diffraction pattern was evaluated by Rietveld method using the Fullprof software. The results indicated single-phase alloy with the MgAgAs-type crystal structure and the cubic lattice parameter $a = 6.3035(1)$ Å, in good agreement with the literature data [6, 7, 10]. Chemical composition of the prepared sample was attested by microprobe analysis to be stoichiometric DyNiSb.

Magnetization and heat capacity measurements were carried out in the temperature range from 1.8 to 300 K in magnetic fields up to 9 T employing Quantum Design MPMS magnetometer and PPMS platform, respectively.

3. Results and discussions

As displayed in the upper inset to Fig. 1, the temperature dependence of the magnetic susceptibility of DyNiSb exhibits a distinct maximum at 3.1 K. This feature indicates the onset of the AFM state, though the phase transition occurs at a somewhat lower temperature than that reported by Karla et al. [11]. The observed difference may arise due to diverse level of crystallographic disorder in the specimens studied.

In the paramagnetic region, the inverse magnetic susceptibility of DyNiSb (Fig. 1.) follows the Curie–Weiss (CW) law, $\chi = C/(T - \theta_{CW})$ with the effective magnetic moment $\mu_{eff} = 10.54(1)$ $\mu_{\rm B}$ and the paramagnetic CW temperature $\theta_{CW} = -11.6(1)$ K. The value of μ_{eff} is close to the magnetic moment of free Dy^{3+} ion (10.63 $\mu_{\rm B}$), and negative θ_{CW} reflects the antiferromagnetic exchange interactions.

The magnetization in DyNiSb is a non-hysteretic function of the magnetic field at any temperature in both the paramagnetic and ordered states. As can be inferred from the lower inset to Fig. 1, below $T_{\rm N}$, the $m(H)$ curve shows a faint change in slope near 1 T, which hints at metamagnetic-like transition from AFM to ferromagnetic (FM) state. At 2 K, the magnetization attains in 9 T a value of 6.7$\mu_{\rm B}$, which is lower than the saturation magnetic moment of Dy^{3+} (10.0 $\mu_{\rm B}$). This substantial reduction can be attributed to crystal field effect.

The AFM phase transition in DyNiSb manifests itself as a distinct peak in the specific heat (Fig. 2.). In applied magnetic fields, the anomaly in $C_p(T)$ broadens and shifts to lower temperatures with increasing field, as ex-

*corresponding author; e-mail: k.synoradzki@int.pan.wroc.pl

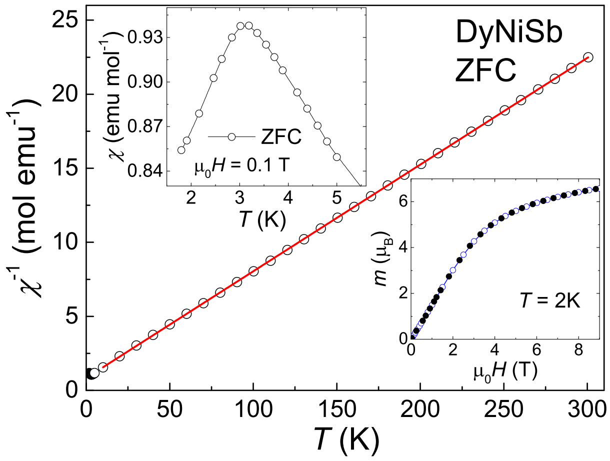

Fig. 1. Temperature dependence of the inverse magnetic susceptibility of DyNiSb measured in a field of 0.1 T. Solid line represents the Curie-Weiss fit. Upper inset: the low-temperature magnetic susceptibility data. Lower inset: magnetic field variation of the ZFC magnetization taken at 2 K with increasing (open symbols) and decreasing (full symbols) magnetic field.

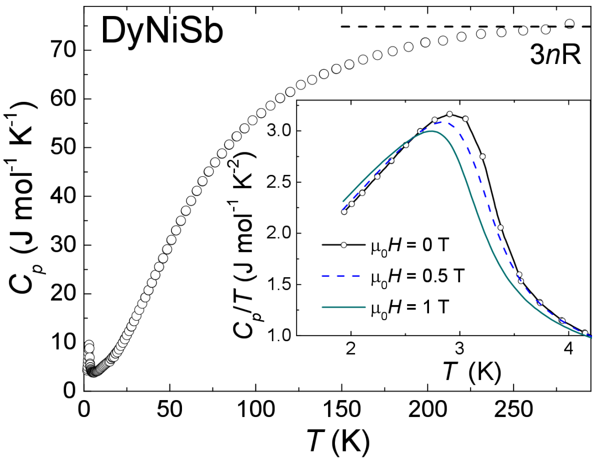

Fig. 2. Temperature dependence of the specific heat of DyNiSb. Dashed line represents the Dulong-Petit limit. Inset: the low-temperature C_p/T data measured in zero and finite magnetic field.

pected for antiferromagnets. Close to room temperature, C_p reaches the Dulong-Petit limit of 74.8 J/(mol K).

To inspect the nature of the phase transition in DyNiSb, the Arrott curves M^2 vs. H/M were plotted (Fig. 3.). Negative slopes observed in weak magnetic fields at $T < T_N$ may suggest a first order character of the phase transition. In turn, positive slopes above T_N are characteristic for a field-induced second order AFM-FM transition.

Figure 4 shows the temperature variations of the magnetic entropy changes in DyNiSb, calculated using the Maxwell relation, $\Delta S_m(T,H) = \int_0^H (\partial M/\partial T)\,\mathrm{d}H$, for magnetic field changes up to 3 T. For small $\Delta\mu_0 H$ values, $-\Delta S_m(T)$ forms at low temperatures a negative narrow minimum, characteristic of inverse magnetocaloric effect

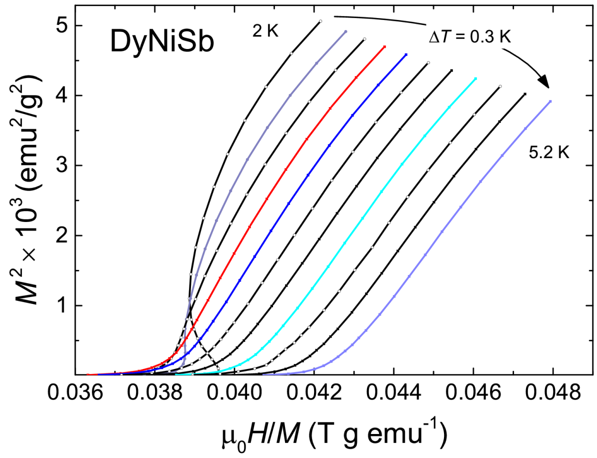

Fig. 3. Arrott plot of DyNiSb at temperatures near T_N.

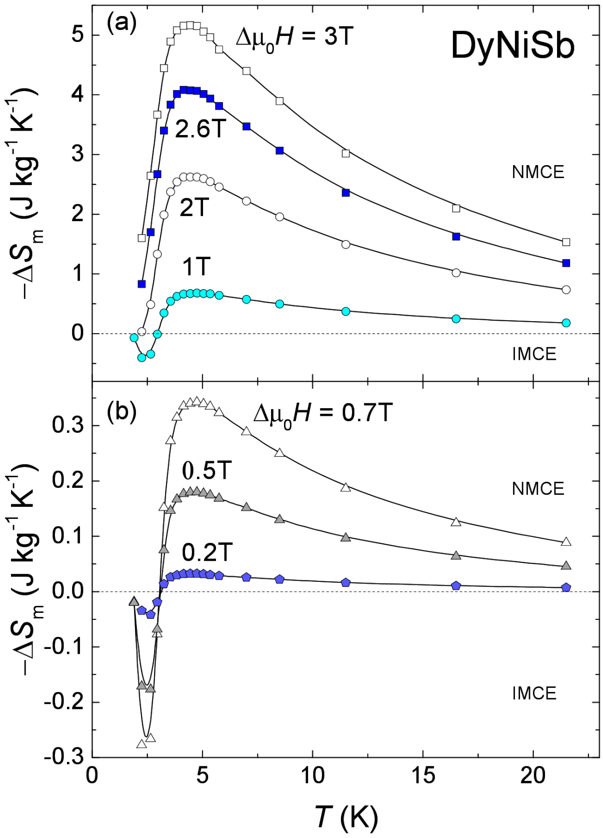

Fig. 4. Magnetic entropy changes in DyNiSb as functions of temperature for (a) $\Delta\mu_0 H > 1$ T and (b) $\Delta\mu_0 H < 1$ T. NMCE: normal MCE; IMCE: inverse MCE.

(IMCE). IMCE occurs when applied magnetic field decouples some of antiparallel aligned magnetic moments, hence increasing disorder in the system, raising its magnetic entropy, and cooling down the sample. IMCE can be observed in materials with AFM order, spin reorientation, and ferrimagnetic-FM transition [12]. The occurrence of this effect in proper combination with normal

MCE (NMCE) may give rise to significant enhancement in the refrigerant efficiency of MCE device.

In DyNiSb, a crossover from IMCE to conventional NMCE occurs around $T_{\rm N}$, and IMCE disappears for $\Delta\mu_0 H > 2$ T. The behaviour observed in the paramagnetic state is typical for field-induced parallel alignment of the magnetic moments. The magnitude of NMCE in the compound studied is larger than that of IMCE. The maximum value of $-\Delta S_m$ is plotted in Fig. 5 as a function of magnetic field for selected temperatures. The highest value of $-\Delta S_m = 5.2$ J/(kg K) was observed at $T = 4.8$ K for $\Delta\mu_0 H = 3$ T. On the same isotherm, $-\Delta S_m = 2.6$ J/(kg K) for $\Delta\mu_0 H = 2$ T.

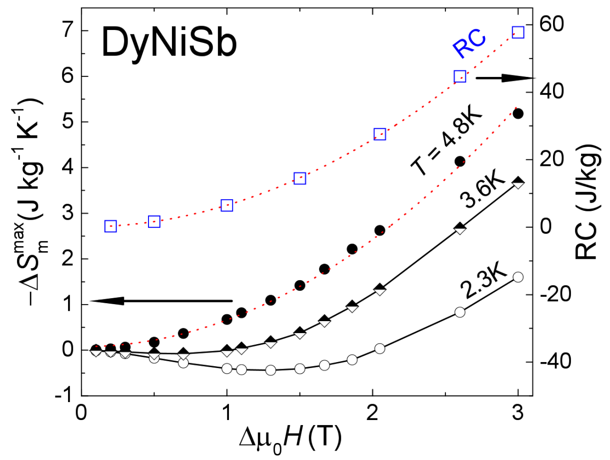

Fig. 5. Maximum value of the entropy change (left axis) and the refrigeration capacity (right axis) of DyNiSb as functions of the magnetic field change for selected temperatures. Dotted lines represent H^2 dependence fit. Solid lines are guides for the eye.

The refrigeration capacity (RC), which is a measure of the amount of heat transferred between the cold and hot reservoirs in an ideal refrigerant cycle, can be calculated by multiplying $|\Delta S_{max}|$ by the full-width-at-half-maximum of the $-\Delta S_m(T)$ variation. For DyNiSb, RC reaches about 58 J/Kg for $\Delta\mu_0 H = 3$ T. As can be inferred from Fig. 5, above $T_{\rm N}$, both $-\Delta S_m$ and RC are proportional to H^2, in a manner typical for paramagnets [13].

The adiabatic temperature change ΔT_{ad} in DyNiSb was calculated using the $-\Delta S_m(T)$ curves (Fig. 4) and the zero field specific heat data (Fig. 2). The temperature variations of ΔT_{ad} (not shown here) were found very similar to $\Delta S_m(T)$. The maximum value of $\Delta T_{ad} = 2.7$ K was obtained for $\Delta\mu_0 H = 3$ T. For $\Delta\mu_0 H = 2$ T, the ΔT_{ad} value was 1.3 K.

4. Conclusions

The arc-melted sample of the half-Heusler alloy DyNiSb was found to order antiferromagnetically at $T_{\rm N} = 3.1$ K. The Arrott plots suggested a slightly first order character of the AFM phase transition. Due to the observed metamagnetic-like transition, the appearance of both normal and inverse magnetocaloric effect was encountered. The largest values of $-\Delta S_m$, ΔT_{ad} and RC, obtained for $\Delta\mu_0 H = 3$ T, were equal to 5.2 J/(kg K), 2.7 K, and 58 J/kg, respectively. The magnitude of MCE derived for DyNiSb is rather modest, yet comparable to those reported for most intermetallics at low temperatures.

Acknowledgments

This work was supported by the National Science Centre under research grant no. 2015/18/A/ST3/00057.

References

[1] T. Toliński, M. Falkowski, A. Kowalczyk, K. Synoradzki, *Solid State Sci.* **13**, 1865 (2011).

[2] T. Toliński, M. Falkowski, K. Synoradzki, A. Hoser, N. Stüßer, *J. Alloys Compd.* **523**, 43 (2012).

[3] M. Falkowski, A. Kowalczyk, T. Toliński, *J. Magn. Magn. Mater.* **331**, 144 (2013).

[4] K. Synoradzki, W. Kowalski, M. Falkowski, T. Toliński, A. Kowalczyk, *Acta Phys. Pol. A* **126**, 162 (2014).

[5] H. Zhang, Y. Li, E. Liu, Y. Ke, J. Jin, Y. Long, B. Shen, *Sci. Rep.* **5**, 11929 (2015).

[6] I. Karla, J. Pierre, B. Ouladdiaf, *Phys. B Condens. Matter* **253**, 215 (1998).

[7] I. Karla, J. Pierre, R.. Skolozdra, *J. Alloys Compd.* **265**, 42 (1998).

[8] J. Pierre, I. Karla, *J. Magn. Magn. Mater.* **217**, 74 (2000).

[9] R. Rawat, I. Das, *J. Phys. Condens. Matter* **13**, L379 (2001).

[10] R.V. Skolozdra, A. Guzik, A.M. Goryn, J. Pierre, *Acta Phys. Pol. A* **92**, 343 (1997).

[11] I. Karla, J. Pierre, A.P. Murani, M. Neumann, *Phys. B Condens. Matter* **271**, 294 (1999).

[12] D.X. Li, T. Yamamura, S. Nimori, Y. Homma, F. Honda, D. Aoki, *Appl. Phys. Lett.* **102**, 152409 (2013).

[13] V. Franco, J.S. Blázquez, A. Conde, *Appl. Phys. Lett.* **89**, 222512 (2006).